

Investigation of Some Characteristics of Polyhydroxy Milkweed Triglycerides and Their Acylated Derivatives in Relation to Lubricity

Rogers E. Harry-O'kuru,^{*,†} Girma Biresaw,[†] Steven C. Cermak,[†] Sherald H. Gordon,[‡] and Karl Vermillion[#]

[†]Bio-Oils Research Unit, [‡]Plant Polymer Research Unit, and [#]Functional Foods Research Unit, National Center for Agricultural Utilization Research, Agricultural Research Service, U.S. Department of Agriculture, 1815 North University Street, Peoria, Illinois 61604, United States

ABSTRACT: Most industrial lubricants are derived from nonrenewable petroleum-based sources. As useful as these lubricants are, their unintended consequences are the pollution of the Earth's environment as a result of the slow degradation of the spent materials. Native seed oils, on the other hand, are renewable and are also biodegradable in the environment, but these oils often suffer a drawback in having lower thermal stability and a shorter shelf life because of the intrinsic $-C=C-$ unsaturation in their structures. This drawback can be overcome, yet the inherent biodegradative property retained, by appropriate derivatization of the oil. Pursuant to this, this study investigated derivatized polyhydroxy milkweed oil to assess its suitability as lubricant. The milkweed plant is a member of the Asclepiadaceae, a family with many genera including the common milkweeds, *Asclepias syriaca* L., *Asclepias speciosa* L., *Asclepias tuberosa* L., etc. The seeds of these species contain mainly C-18 triglycerides that are highly unsaturated, 92%. The olefinic character of this oil has been chemically modified by generating polyhydroxy triglycerides (HMWO) that show high viscosity and excellent moisturizing characteristics. In this work, HMWO have been chemically modified by esterifying their hydroxyl groups with acyl groups of various chain lengths (C2–C5). The results of investigation into the effect of the acyl derivatives' chemical structure on kinematic and dynamic viscosity, oxidation stability, cold-flow (pour point, cloud point) properties, coefficient of friction, wear, and elastohydrodynamic film thickness are discussed.

KEYWORDS: Asclepiadaceae oil, polyhydroxy triglycerides, polyacyl triglycerides, rheology, cold-flow properties, film thickness, coefficient of friction, wear scar dimensions, lubricity

INTRODUCTION

The common milkweed (*Asclepias syriaca* L.) and its related species have traditionally been viewed by most farmers who have encountered it with nonsalutary names such as “the wheat farmer's nightmare” and “nuisance”. This attitude was based on the unwelcome effect of milkweed released floss on crop-harvesting equipment. Ironically, the floss was the plant component that made milkweed “A War Strategic Material” for the Pacific theater of World War II.¹ Although the plant is native to the Americas from coast to coast, its modest commercial use has been confined to application of its hypoallergenic seed floss as a fiber-fill in high-end pillows, comforters, and jacket linings. The milkweed seed itself found no more use other than for highway beautification and butterfly nursery plantings. Utilization of the main seed resources (oil and phytochemicals) had hitherto been hardly explored. The seeds contain a highly unsaturated (92%) oil that is 25–30% by weight of the dry seed. Therefore, in a continued effort to tap the enormous potential of this oil we have exploited its polyolefinic character to generate its polyoxirane derivatives.^{2,3} Ring-opening of these oxiranes afforded the polyhydroxy triglycerides (HMWO) of the oil, a castor-like product without the unsaturation. Like castor, the HMWO and their precursor epoxidized milkweed oil platform open several synthetic avenues for the preparation of otherwise inaccessible but important personal-care and industrial materials.^{4–6} Stemming from the previously observed high viscosity of the HMWO, we have in this study explored potential use of the HMWO as lubricants via esterification of their hydroxyl functionalities with acyl groups of various chain lengths. The obtained acyl derivatives of HMWO were

positively identified by FT-IR and NMR. The polyacyl triglycerides obtained were then investigated for their lubricant properties such as cold-flow properties (pour points and cloud points), oxidative stability using a rotating pressurized vessel oxidation test (RPVOT), viscosity, viscosity index, elastohydrodynamic (EHD) film thickness, friction, and wear on a four-ball tribometer. This paper details the results of these investigations.

MATERIALS AND METHODS

Materials. Milkweed oil (MWO) was obtained from Natural Fibers Corp. (Ogallala, NE), whereas sodium chloride, sodium bicarbonate, ethyl acetate, hexane, and acetic, butyric, and valeric anhydrides were purchased from Acros Organics (Chicago, IL); 4-dimethylaminopyridine (4-DMAP) and anhydrous magnesium sulfate were from Sigma-Aldrich (St. Louis, MO). Milkweed HMWO were synthesized from cold-pressed MWO as described previously.⁴ All chemicals and solvents were of reagent grade and were used as supplied.

Test balls used in four-ball antiwear (4-ball AW) experiments were obtained from Falex Corp. (Aurora, IL) and had the following specifications: chrome–steel alloy made from AISI E52100 standard steel; 64–66 Rc hardness; 12.7 mm diameter; grade 25 extra polish. The test balls were degreased by two consecutive 5 min sonications in isopropyl alcohol and hexane solvents in an ultrasonic bath before use in the 4-ball AW experiments.

Received: September 2, 2010

Revised: February 22, 2011

Accepted: February 23, 2011

Published: March 23, 2011



Methods. Instrumentation. (a) *FT-IR Spectrometry.* FT-IR spectra were measured on an Arid Zone FT-IR spectrometer (ABB MB-Series, Houston, TX) equipped with a DTGS detector. Liquid derivatives were pressed between two NaCl disks (25 mm × 5 mm) to give thin transparent oil films for analysis by FT-IR spectrometry. Absorbance spectra were acquired at 4 cm⁻¹ resolution and signal-averaged over 32 scans. Interferograms were Fourier transformed using cosine apodization. Spectra were baseline corrected, scaled for mass differences, and normalized to the methylene peak at 2927 cm⁻¹.

(b) *NMR Spectroscopy.* ¹H and ¹³C NMR spectra were acquired on a Bruker AV-500 MHz Spectrometer with a dual 5 mm proton/carbon probe (Bruker, Ballerica, MA). The internal standard used was tetramethyl silane.

Viscosity Measurements. Viscosities were determined on a Temp-Trol constant-temperature bath (Precision Scientific, Chicago IL) using a Cannon-Fenske viscometer for transparent liquids (Cannon Instrument Co., State College, PA) in accordance with AOCS Official Method Tq 1a-64.⁷ The size of the Cannon-Fenske viscometer used was number 500. The cleaned dry tube was loaded at room temperature (RT) with the sample oil and placed in its holder in the constant-temperature bath. The sample was allowed to equilibrate for 10 min at 40 °C or for 15 min at 100 °C before the sample was suctioned into the lower bulb until the meniscus just overshot the mark above the lower bulb.

The suction was removed and the meniscus adjusted to the mark. The sample was allowed to flow at the same time the stop clock was started. The time (in seconds) it took the meniscus to reach the mark below the bulb multiplied by the tube constant gave the viscosity of the sample. All kinematic viscosity measurements were run in duplicate, and the average values are reported.⁸

Dynamic viscosity at 40 and 100 °C was directly measured on an ARES LS-2 rheometer (TA Instruments Waters LLC, New Castle, DE) as described elsewhere.⁹ Viscosity indices (VIs) were calculated from the kinematic viscosity data at 40 and 100 °C following the procedure outlined in ASTM D2270.¹⁰

Densities. Density measurements were performed using a pycnometer or Kimble Specific Gravity Bottle (10 mL) equipped with a thermometer (Kimble Glass Inc., Vineland, NJ). The pycnometer was cleaned with acetone and dried with an air jet at RT. The components were reassembled and weighed empty. Each sample was carefully introduced into the bottle until the liquid meniscus grazed the lower portion of the ground glass joint. The thermometer lid was carefully inserted, allowing any excess sample to exit through the open side arm. The completely filled pycnometer was carefully cleaned of excess sample, the side arm cap replaced, and the system then weighed at the operating RT. The difference in mass from the empty pycnometer mass is the mass of 10.0 mL of sample. Two replicates for each sample were measured from which an average mass of sample was derived. Between samples, the pycnometer assembly was thoroughly rinsed with a mixture of hexane/acetone and dried before reuse.

Acetylation of HMWO. HMWO (95.5 g, 92.3 mmol) were placed in a flame-dried round-bottom flask (RBF) equipped with a magnetic stir bar. Acetic anhydride (94.23 g, 100 mL) and 4-DMAP (2.0 g) were added and stirred at RT for 24 h. The reaction mixture was then poured into a stirring saturated NaHCO₃ solution; stirring was continued until effervescence ceased. The aqueous mixture was extracted with EtOAc (150 mL × 3); the combined extract was dried over anhydrous MgSO₄ and concentrated under reduced pressure at 57 °C. The concentrate was redissolved in ethyl acetate and heated close to boiling, activated charcoal was added, and then the mixture was reheated to the boil for 2 min. After filtering, the filtrate was again reheated, and 2.0 g of acid-washed clay was added and heated to a boil. The mixture was filtered and concentrated at 57 °C under reduced pressure to yield 121.7 g (90.6%). The FT-IR spectrum of a sample of this derivative on NaCl disk gave

$\nu_{\text{film}} \text{ cm}^{-1}$ 2928, vs, 2857 s, 1741 vs, 1463 m, 1372 s, 1235 vs, 1171 s, 1026 s, 949 w, 725 w. Its density at 21.8 °C was 1.14 g cm⁻³, and its kinematic viscosity at 40 °C was 1733.6 cSt and was 78 cSt at 100 °C, that is, a viscosity index (VI) value of 105.0. ¹H NMR (CDCl₃) δ 4.3 m (3H), 4.25 m (5H), 2.30 t (J = 7.3 Hz, 7.4 Hz, 8H), 2.05 s (15H), 1.55 m (22H), 1.30 m (68H), 0.84 t (J = 6.8 Hz, 5.0 Hz, 12H); ¹³C NMR (CDCl₃) δ 173.23, 173.20, 173.14, 172.74, 171.08, 170.55, 170.51, 170.46, 170.36 (C=O); 160.51 (C=C of 4-DMAP); 81.73, 81.66, 81.19, 81.09, 81.02, 80.92, 77.64, 75.10, 75.04 (-CHO- on the triglyceride chains); 68.88 (-CHO- backbone methine carbon on glycerol); 63.71 (-CH₂O-); 62.77 (-CH₂O-); 60.83 (-CH₂O-); 35.49, 34.29, 34.08, 34.00, 33.97, 33.92 (-CH₂ proximal to the carbonyl groups); 31.88, 31.78, 31.62, 31.53, 31.17, 27.82, 26.59, 26.30, 26.12, 25.86, 25.79, 22.45(2) (-CH₂); 21.12, 21.03, 20.95, 20.93, 20.80, 20.69, 20.55 (-CH₃ of acetate); 14.21, 14.12, 14.10, 14.03, 13.99 (terminal CH₃ of triglycerides).

Butyroylation of HMWO. Butyric anhydride (310 g, 1.941 mol) and 4-DMAP (2.0 g) were added to polyhydroxy MWO (203.0 g, 196.2 mmol) in a 500 mL RBF. The reaction mixture was stirred and gently heated to 45 °C. The reaction was monitored by TLC on a precoated silica gel (20 × 5 cm) plate using hexane/ethyl acetate/acetic acid (7:5:1) solvent. The reaction was stopped after 26 h when TLC showed complete consumption of the starting material. The product showed a more defined R_f = 0.85–0.96 compared to the smeared trace of the HMWO starting material. The product mixture was poured into a saturated NaHCO₃ solution and stirred until effervescence stopped. The aqueous mixture was then extracted with EtOAc (300 mL × 3), and the combined dark amber colored extract was heated to near boiling; activated carbon was added and allowed to boil. The mixture was hot filtered and the filter cake rinsed with more EtOAc. This filtrate was again heated with 2.5 g of clay (Nevergreen). The mixture was filtered and dried over Na₂SO₄ and concentrated at 57 °C under reduced pressure to yield 250.7 g (73.6% of theoretical) of viscous oil. The FT-IR spectrum of a sample of this material on NaCl disk gave $\nu_{\text{film}} \text{ cm}^{-1}$ 2926 vs, 2858 s, 1818 w, 1737 vs, 1461 m-s, 1373 m-s, 1251 s, 1170 vs, 1096 s, 1035 m-s, 725 w. Its kinematic viscosity was 926.2 cSt at 40 °C and 63.2 cSt at 100 °C, that is, a VI of 131.0. Its density at 21.8 °C was 1.11 g·cm⁻³; specific gravity 1.1103. ¹H NMR (CDCl₃) δ (ppm): 5.2 (residual olefin), 4.36 m (6H), 4.3 m (3H), 3.9 m (2H), 2.3 m (24H), 1.66 m (44H), 1.29 bs (86H), 0.95 (overlapping triplets of terminal methyl groups of butyroyl substituents, 21H) and 0.86 m (overlapping triplets of methyl groups of triglycerides, 15H). ¹³C NMR (CDCl₃) δ 173.24, 173.20, 173.14, 173.10, 172.74, 171.08 (C=Os); 160.0 (C=C of 4-DMAP); 74.99, 74.90, 74.78, 74.76, 74.69, 74.66, 74.02, 73.75, 73.54, 73.51, 73.15, 73.11, 70.50 (CHO- of the hydroxylated triglyceride chains); 68.92 (-CHO- of the glyceride backbone); 63.76, 62.09, 60.39 (-CH₂O- of glycerol backbone); 33.97, 33.93, 31.88, 31.78, 31.58, 30.76, 30.66 (-CH₂ next to carbonyls); 29.66, 29.62, 29.43, 29.36, 29.32, 29.30, 29.23, 29.13, 29.08, 29.04, 29.00, 28.95, 28.93; 25.09, 24.79, 24.73, 20.98 (-CH₂-); 18.57, 18.55, 18.52, 18.46, 18.41, 17.74 (-CH₂ contiguous to terminal -CH₃ of butyrate substituents); 14.16, 14.07, 14.04 (-CH₃ of triglyceride); 13.98, 13.95, 13.92, 13.66, 13.64, 13.57 (-CH₃s of substituents).

Valeroylation of HMWO. Valeric anhydride (98%, 200.0 g, 1.052 mol) and 4-DMAP (1.0 g) were added to HMWO (173.9 g, 168.1 mmol). The mixture was stirred and warmed to 40 °C until the hydroxylated groups on the oil had been completely esterified, ca. 24 h. The product mixture was then poured into a saturated NaHCO₃ solution and stirred until neutralized. The neutralized aqueous mixture was extracted with ethyl acetate (300 mL × 3), and the extract was treated with a mixture of charcoal and clay as above and filtered; the filtrate was dried over Na₂SO₄. The solution was filtered and concentrated under reduced pressure to give 224.0 g (78.1% of theoretical). FT-IR spectrum of this product on NaCl disk gave $\nu_{\text{film}} \text{ cm}^{-1}$ 2957 vs, 2931 vs, 2859 s, 1819 w,

1739 vs, 1465 m, 1378 m, 1244 m-s, 1172 s, 1036 s. Its kinematic viscosity was 489.4 cSt at 40 °C and 42.2 cSt at 100 °C, that is, a VI of 136. Its density at 21.8 °C was 1.096 g cm⁻³ and specific gravity, 1.099. ¹H NMR (CDCl₃) δ 4.30 m (3H), 4.10 m (6H), 3.90 m (2H), 2.44 t (*J* = 7.4 Hz, 7.5 Hz, 3H), 2.30 m (23H), 1.55 m (45H), 1.30 m (100H), 0.90 (overlapping triplets of terminal methyls of valeroyl substituents, 24 H), 0.85 (overlapping terminal methyl groups of triglycerides, 15H). ¹³C NMR (CDCl₃) δ 178.22, 173.30, 173.26, 173.22, 173.19, 173.13, 172.72, 171.06, 168.54 (C=Os); 160.51 (C=C of 4-DMAP); 77.27, 74.72 (-CHO-); 68.87 (-CHO- of triglyceride backbone); 63.68 (-CH₂O-), 62.04, 60.33 (-CH₂O-); 34.93, 34.28, 34.20, 34.16, 34.14, 34.12, 34.07, 34.04, 34.00 (α-CH₂- to carbonyls); 33.96, 33.92, 33.84, 33.54 (-CH₂s- at C11 between hydroxylated C10 and C12 of the linoleyl chains); 31.14, 31.10, 30.73, 30.64, 29.65, 29.61, 29.57, 29.45, 29.43, 29.35, 29.31, 29.29, 29.22, 29.14, 29.12, 29.07, 29.03, 28.99, 28.94, 28.92, 28.84, 28.78, 27.14, 27.10, 27.05, 27.00, 26.93, 26.84, 26.76, 26.53, 26.22, 25.76, 25.28, 25.25, 25.07, 25.05, 25.03, 24.95, 24.82, 24.78, 24.75, 24.72, 22.64, 22.60, 22.47, 22.44, 22.24, 22.15, 21.96, 20.96 (-CH₂-); 14.15, 14.06, 14.04, 13.97, 13.95, 13.91 (terminal methyl groups of triglycerides); 13.68, 13.64, 13.59 (terminal methyl groups of valeroyl substituents).

Pour Point (PP) Measurements. PP was measured following ASTM method D97-96a¹¹ to an accuracy of ±3 °C. The procedure involves placing a test jar with 50 mL of the sample into a cylinder submerged in a cooling medium. The sample temperature was measured in 3 °C increments at the top of the sample until the material stopped pouring. The sample no longer poured when the material in the test jar did not flow when held in a horizontal position for 5 s. The temperature of the cooling medium was chosen on the basis of the expected PP of the material. Samples with PPs that ranged from +9 to -6 °C, from -6 to -24 °C, and from -24 to -42 °C were placed in baths of temperatures of -18, -33, and -51 °C, respectively. PP is defined as the coldest temperature at which the sample still poured. All PPs were run in duplicate, and averaged values are reported.

Cloud Point (CP) Measurements. CP is determined following ASTM method D2500-99¹² to an accuracy of ±1 °C. The method involves placing a test jar with 50 mL of the sample into a cylinder submerged in a cooling medium. The sample temperature was measured in 1 °C increments at the bottom of the sample until any cloudiness was observed at the bottom of the test jar. The temperature of the cooling medium was chosen on the basis of the expected CP of the material. Samples with CPs that ranged from RT to 10, from 9 to -6 °C, from -6 to -24 °C, and from -24 to -42 °C were placed in baths at temperatures of 0, -18, -33, and -51 °C, respectively. All CP measurements were conducted in duplicate, and average values are reported.

Rotating Pressurized Vessel Oxidation Test (RPVOT). RPVOT experiments were conducted on an apparatus manufactured by Koehler, Inc. (Bohemia, NY) using ASTM method D 2272-98.¹³ A commercial antioxidant package, LZ 7652 (The Lubrizol Corp., Wickliffe, OH), was blended into the test oil samples on a % w/w basis. Formulated samples were stirred for 24 h before use in RPVOT experiments. All RPVOT experiments were conducted at 150 °C. The copper catalyst used in the experiments was 3 m long and sanded with 220 grit silicon carbide sand paper produced by Abrasive Leaders and Innovators (Fairborn, OH) and was used immediately. The wire was wound to have an outside diameter of 44–48 mm, a height of 40–42 mm, and a weight of 55.6 ± 0.3 g. In a typical experiment, 50.0 ± 0.5 g of blended samples was weighed into the pressure vessel, to which 5.0 mL of reagent grade water and the freshly prepared catalyst copper wire were added. The vessel was then assembled and slowly purged with reagent grade oxygen twice. The pressure vessel was charged with 90.0 ± 0.5 psi (620 kPa) of reagent grade oxygen and then checked for oxygen leaks by immersing the vessel in water. The test began after the absence of leaks had been confirmed and was stopped and the time recorded when the pressure in the vessel dropped by 175 kPa from the

maximum pressure. All samples were run in duplicate, and the average RPVOT times in minutes are reported.

Friction and Wear Measurements. Friction and wear tests were conducted using a four-ball tribometer (model KTR-30 L, Koehler Instruments) following the 4-ball AW test method ASTM D 4172-94¹⁴ under the following test conditions: load, 392 ± 2 N (40 ± 0.2 kgf); speed, 1200 ± 40 rpm; lubricant temperature, 75 ± 2 °C; test duration, 60 ± 1 min. During the test, the torque required to overcome the friction opposing the rotation of the ball was continuously measured and recorded along with the spindle speed, load, and lubricant temperature. The measured frictional torque was converted into a coefficient of friction (COF) following the procedure outlined in ASTM method D5183-95.¹⁵ At the end of the test period, the wear scar diameter (WSD) on each of the three bottom balls was measured along and transverse to the wear direction using an automated wear scar measurement system, comprising hardware and software (Scar View software version 2005, Koehler Instruments).

The four-ball instrument load and torque cells were properly calibrated prior to use, and freshly degreased test balls were used in each test. In a typical experiment, the rotating ball was first secured in the collet of the top spindle. The three stationary balls were secured in the pot using a wrench set to the recommended pressure. The test lubricant was then poured into the pot until the balls were completely submerged. The assembled ball pot was then placed in the tribometer and the load applied carefully so the top ball contacted all three bottom balls. The test parameters (lubricant identification, speed, load temperature, duration) were entered into the computer, and the heater was turned on. The test started automatically, as soon as the test temperature was reached, and continued until the test duration expired. At the end of the test, the ball pot was removed, the oil was poured out, the pot and balls were rinsed with hexanes, and the WSDs of the three balls were measured. For each test lubricant, two antiwear tests were conducted using fresh balls and test lubricants. The COFs and WSDs from the two tests were averaged and used in further analysis.

Film Thickness. Lubricant film thickness was measured using the optical interferometry method between a glass disk and a steel ball. Details regarding the basic principles of the optical interferometry method can be found elsewhere.¹⁶ Film thickness measurement was conducted on an EHL Ultrathin Film Measurement System (PCS Instruments, London, U.K.). The glass disk used with this instrument is coated with a semireflecting chrome layer, which is coated with a silica spacer layer of predetermined thickness to allow for instrument calibration as well as for measuring very thin (ultrathin) lubricant films. The EHL Ultrathin Film Measurement System (PCS Instruments) has several components including a mechanical unit, an electronic unit, an optical system, and a computer with the appropriate software. A detailed description of the main components has been given previously.¹⁷ The specifications of the instruments are as follows: disk, 100 mm diameter by 12 mm thick float glass, coated with ~20 nm semireflecting chrome layer, which in turn is coated with ~500 nm thick silica spacer layer; precision steel ball, superfinished ³/₄ in. diameter, G10 carbon Cr steel (AISI 52100); measured film thickness, 1–1000 ± 1 nm; rolling speed, 0–3 m/s; slide-to-roll ratio, 0–200%; applied load, 0–50 N; maximum contact pressure, 0.7–1.1 GPa; lubricant temperature, ambient to 150 °C. In this work, film thickness test parameters were varied as follows: speed, 0.02–3.0 m/s in 20% increments; load, 10–40 N in 10 N increments; temperature, 30, 40, 70, and 100 °C. A detailed description of the procedure for film thickness measurement on the EHL Ultrathin Film Measurement System (PCS Instruments), including instrument setup/calibration and data acquisition/analysis, have been given previously.¹⁷

RESULTS AND DISCUSSION

The HMWO used as the starting material in this investigation Figure 1A was a pale yellow, very viscous liquid as described

A

Esterification of Milkweed Polyhydroxy Triglycerides

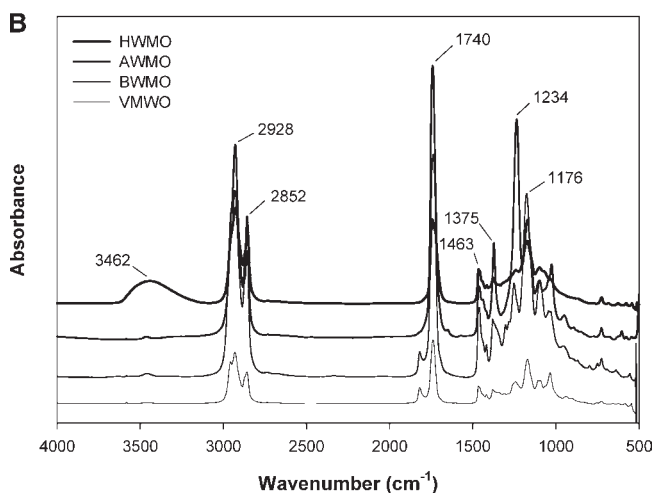
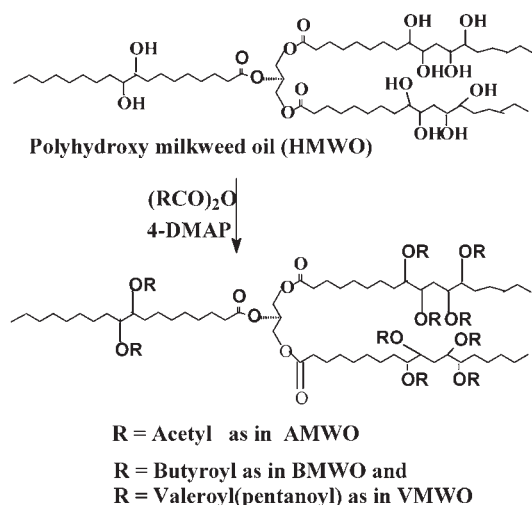


Figure 1. (A) Generation of milkweed polyhydroxy triglycerides and its acyl derivatives from milkweed oil oxiranes. (B) FT-IR spectral overlay of HMWO and its three peracyl derivatives.

previously.^{3,4} The kinematic and dynamic viscosities of its acyl derivatives from which the VIs were calculated are summarized in Tables 1 and 2. An earlier constitutive modeling study of the rheology of HMWO had indicated this oil exhibited non-Newtonian viscoelastic behavior, which could be explained by the presence of the many hydroxyl groups in its structure that would naturally form intermolecular hydrogen bonds and thus show unusual flow behavior at lower temperatures.¹⁸ The FT-IR spectrum of the HMWO is characterized by a prominent broad band centered at 3462 cm^{-1} , which is attributable to hydrogen-bonded O–H stretching frequencies as a consequence of the multiple hydroxyl group content of this starting material (Figure 1B). In contrast, one of the first noticeable IR spectral features observed in each peracylated derivative is the disappearance of the hydroxyl stretching mode (3600–3200 cm^{-1} , Figure 1B). This is expected from substitution of the hydroxyl protons of the secondary alcohols of the triglyceride chains by the esterifying substituent acyl moieties. The other notable features of the FT-IR spectra are the prominence of the alkyl and carbonyl

Table 1. Kinematic Viscosity and Viscosity Index (VI) of Selected Seed Oils and Milkweed and Derivatives with Densities of Milkweed Derivatives

oil ^a	kinematic viscosity (cSt)			VI ^c	density 21.8 °C ^a
	25 °C	40 °C ^b	100 °C ^b		
MWO		33.8	7.3	210	<1
SBO ^d		31	7.6	227	
CANO ^d		34	7.8	215	
ESBO	420 ^e	170.9	20.4 ^f		
EMWO		164.4	19.22	133	1.05 (23 °C)
HMWO		2332	75.5	85	1.14 (24.2 °C)
AMWO		1733	78	105	1.14
BMWO		926.2	63.2	131	1.11
VMWO		489.4	42.2	136	1.10

^aMWO. ^bASTM D2270, using Cannon-Fenske viscometer according to AOCS official method Tq 1a-64. ^cVI measured according to ASTM method D 2770. ^dData for soybean oil (SBO) and canola (CAN) obtained using ASTM method D 2770, Lawate.¹⁹ ^eTechnical Information, Vikoflex 7170 Epoxidized Soybean Oil, Arkema Inc., 2010 (from the web: www.arkema-inc.com). ^fAdhvaryu and Erhan.²⁰

Table 2. Dynamic Viscosity of Selected Seed Oils versus Milkweed Derivatives (mPa-s)

oil ^a	40 °C ^a	70 °C ^a	100 °C ^a
MWO	33.8		7.3
SBO ^b	30.3		7.3
CANO ^b	33.3		7.0
HMWO	31,986 ^c	494.6 ± 13.7	103.1 ± 5.5
HMWO		482.3 ± 29.6	105.6 ± 5
AMWO	1360.6 ± 14.1	308.1 ± 15.1	96.8 ± 5.8
AMWO		300.1 ± 10.8	97.4 ± 5.3
BMWO			
VMWO			

^aMeasured on TA Instruments ARES LS1 controlled strain rheometer at 0.1–100 s^{-1} shear rate using a 50 mm cone and plate geometry, cone angle of 0.0401 radian, and gap of 0.046 mm. ^bDynamic viscosity of soybean oil (SBO) and canola (CAN) from ref 17. ^cThe sample was non-Newtonian at 40 °C, and the viscosity was obtained by analyzing the data using the Cross model.

frequencies around 2940–2850 and 1740 cm^{-1} , respectively, resulting from the substituent moieties' contribution to the spectrum.

The NMR spectra of these derivatives are shown in Figure 2. The ¹NMR of the AMWO is given in Figure 2a, and the ¹³C NMR of the acyl derivatives are shown in Figure 2b–d. The most informative NMR spectra are obtained from stacking the distortionless enhancement proton transfer experiments (DEPT) of the ¹³C spectra (Figure 2e) of the three derivatives. This allowed the substituent terminal methyl groups to be unambiguously distinguished from those of the parent triglyceride in each derivative. For instance, in Figure 2e, entry spectrum A is the polyacetyl triglyceride (AMWO) in which the methyl groups of the substituent acetyl units are chemically shifted downfield to around 21 ppm compared to the terminal methyl groups of the parent triglycerides, which resonate at around 14 ppm. This is

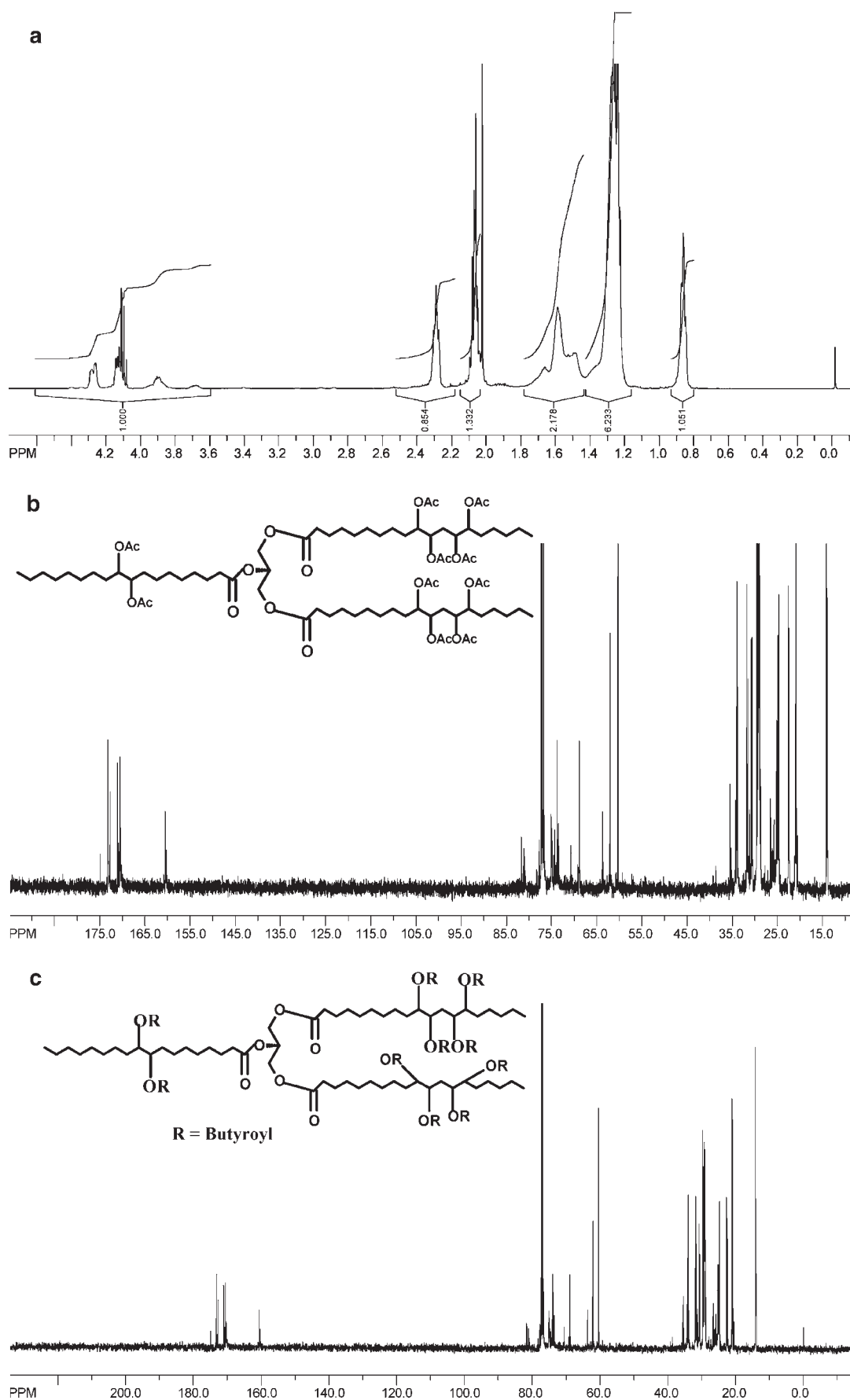


Figure 2. Continued

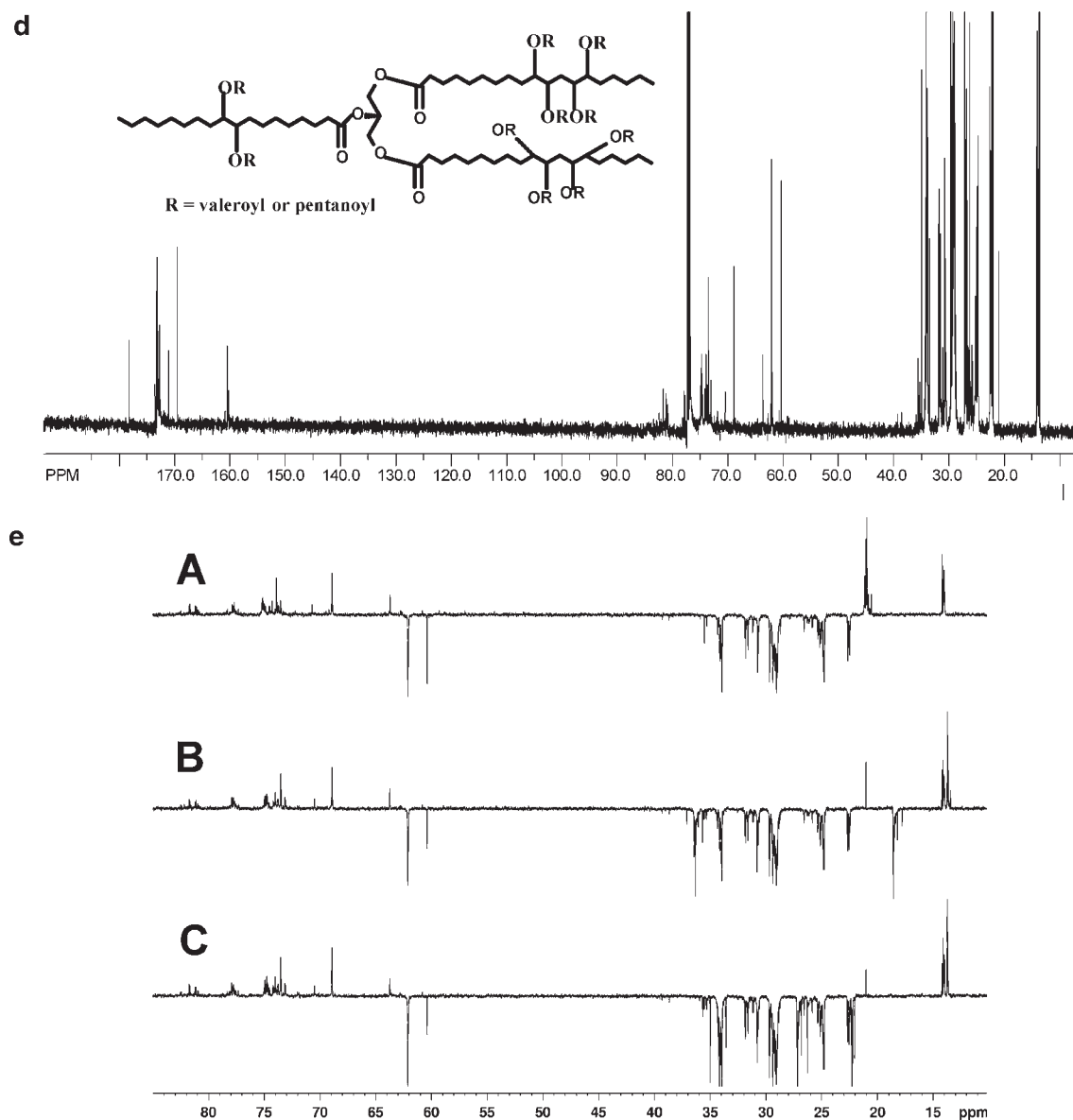


Figure 2. (a) ^1H NMR of peracetyl polyhydroxy triglyceride derivative of milkweed oil. (b) ^{13}C NMR of peracetyl polyhydroxy triglyceride derivative of milkweed oil. (c) ^{13}C NMR of perbutyryl polyhydroxy triglyceride derivative of milkweed oil. (d) ^{13}C NMR spectrum of the pervaleroyl derivative of polyhydroxy triglyceride of milkweed oil. (e) ^{13}C NMR DEPT spectra of the peracetyl (A), perbutyryl (B), and pervaleroyl (C) derivatives of milkweed polyhydroxy triglycerides.

understandable from the deshielding effect of the contiguous carboxyl $\text{C}=\text{O}$ on the acetate methyl carbon. In contrast, the terminal methyl groups of the longer chain substituents, which are farther removed from this influence in the butyryl and pentanoyl substituents, resonate at higher field (around 13 ppm) from the terminal methyl groups of the parent triglyceride and are observed consistently at around 14 ppm in all derivatives. An additional noticeable point in the butyryl derivative, entry B, is that the methylene groups next to the terminal carbons resonate at a higher field of around 18 ppm compared to the equivalent methylene groups in the pentanoyl derivative. This observation is consonant with the spectra of butyryl esters, but it bears mentioning here. Another feature of both the proton NMR and the infrared spectra of these acyl derivatives is that neither

technique indicates the presence of residual hydroxyl groups in the polyacylated derivatives of HMWO.

Kinematic Viscosity. The kinematic viscosity of MWO and its acyl derivatives at 40 and 100 °C is summarized in Table 1. For purposes of comparison, literature viscosity and VI values for soybean (SB) and canola (CAN) oils and derivatives are also included in Table 1. MWO displayed average kinematic viscosities of 33.8 and 7.3 cSt at 40 and 100 °C, respectively. These viscosity values are slightly higher than those for SB or CAN oils (Table 1). This may have to do with differences in the degree of purification between these three oils. Epoxidation resulted in a large increase in the kinematic viscosity of EMWO. An even greater, almost 50-fold, increase in kinematic viscosity was observed for the HMWO derivative. This

increase in viscosity of HMWO is attributable to a high degree of intermolecular H-bonding between HMWO molecules. Esterification of HMWO, however, resulted in a reduction of kinematic viscosity (Table 1). The degree of attenuation in viscosity of esterified HMWO was a function of the substituent group chain length.

The VI of unmodified MWO is 210, which is slightly lower than the values for SB and CAN oils, but within the range expected of seed oils.¹⁹ Epoxidation and esterification resulted in a dramatic decrease in the VI of milkweed oil. For example, the VI of HMWO was 85, which improved slightly with esterification. The VI of esterified HMWO increased with increasing chain length of the substituent group.

Dynamic Viscosity. The dynamic viscosities of MWO and derivatives were measured on an ARES LS1 controlled strain rheometer (TA Instruments, New Castle, DE) at 40, 70, and 100 °C. Measured viscosities are summarized in Table 2. Data for SB and CAN oils have been included in Table 2 for comparative purposes. The dynamic viscosities of MWO at 40 and 100 °C were 33.8 and 7.3, respectively, which are within the range reported for SB, CAN, and other seed oils.¹⁹ HMWO displayed a very high dynamic viscosity (~1000-fold relative to MWO) and non-Newtonian behavior at 40 °C. At 70 °C or higher temperatures, however, it displayed Newtonian behavior. The latter behavior confirms the strong intermolecular hydrogen-bonding resulting in non-Newtonian behavior of this compound at lower temperatures. Higher temperatures, therefore, thermally disrupted these intermolecular hydrogen bonds, freeing the molecules to behave as a Newtonian fluid. Esterification similarly disrupts hydrogen bonding; hence, the dynamic viscosities of the esterified HMWOs decreased with increasing ester group chain length as observed: HMWO \gg AMWO > BMWO > VMWO. This trend was observed for data generated at all temperatures. Analogous observations of the effect of branching on viscosity had been reported in branched polysaccharides,²¹ branched synthetic polymers,^{22–25} and oligomerized estolides of oleic acid.²⁶

Cold Flow. The PPs and CPs of MWO and derivatives are summarized in Table 3 with PP values for SB and CAN oils and similar derivatives of SB oil included. HMWO displayed similar PP as hydroxy soybean oil (HSBO), which showed improvement over SBO. AMWO displayed similar PP as ASBO, which was higher than HSBO, HMWO, and even SB oil. BMWO and VMWO displayed similar PPs that were identical to that of HMWO. However, the PP of BSBO (−3 °C) was identical to those of ASBO and AMWO but much higher than that of BMWO (−18 °C). This result is clearly anomalous because almost all SB oil and MWO derivatives displayed similar PP values except for BMWO and VMWO. The CP of HMWO displayed a 4-fold improvement upon esterification. There were no effects of ester group chemical structure on CP. The esterified HMWO derivatives had CPs that were in the range from −25 to −28 °C.

Oxidation Stability (OS). The OS data for MWO and derivatives, which were obtained using the RPVOT method, are summarized in Table 4. OS evaluations were conducted on samples with (3.5% w/w) and without blended commercial antioxidant additives. For comparison, similar literature data for CANO and SBO are included in Table 4. As can be seen, MWO derivatives (HMWO, etc.) without antioxidant additives displayed slight improvements in OS compared to unmodified SB or CAN oils. On the other hand, samples containing

Table 3. Low-Temperature Flow Properties of Soybean (SBO), Milkweed (MWO), and Derivatives

	pour point (°C)	cloud point (°C)	ref
SBO	−9		19
CANO	−21		19
ESBO	3		27
HSBO	−18		27
HMWO	−15	−7	this work
ASBO	−3		27
AMWO	−3	−25	this work
BSBO	−3		27
BMWO	−18	−30	this work
VMWO	−18	−28	this work

Table 4. RPVOT Oxidative Stability Results for Soybean (SBO), Milkweed (MWO), and Derivatives, without and with Blended Commercial Antioxidant Additive Package (min)

	no AO	3.5% comm AO ^a	ref
SBO	13	28	19
CANO	10	43	19
HMWO	15	20	this work
AMWO		74	this work
BMWO	16	67	this work
VMWO		52	this work

^a LZ 7652 from Lubrizol Corp.

the commercial antioxidant additives displayed significant improvements in OS. However, the improvements due to added antioxidant varied and were dependent on the nature of the oil being tested. For HMWO, the oxidation stability improved from 15 min without to 20 min with added antioxidant. For the polyacyl compounds (AMWO, BMWO, VMWO), however, the changes were more significant; up to a 4-fold increase in RPVOT times was observed. A closer examination of the OS data indicated that, for the MWO derivatives, the oxidative stability seems to decrease with increasing acyl substituent chain length.

EHD Film Thickness. Film thickness was investigated using the optical interferometry method. Film thickness was measured as a function of lubricant entrainment speed, temperature, and applied load. In these studies, only the acetylated (AMWO) and valerylated (VMWO) milkweed esters were investigated. These two oils were chosen because they had the highest and lowest viscosities, respectively, among the three milkweed esters investigated in this work (Tables 1 and 2). Also, HMWO was not investigated because it was far too viscous for the measurement system. A typical data set from film thickness measurement by optical interferometry is illustrated in Figure 3. The data in Figure 3 are for VMWO, but similar data were also obtained for AMWO. AMWO and VMWO oils displayed the familiar entrainment speed versus film thickness profiles displayed by lubricating oils. The film thickness increased with increasing entrainment speed and decreasing temperature. This is illustrated by the data in Figure 3, which compares the film thickness of VMWO as a function of entrainment speed at 40 and 70 °C. The data in Figure 3 were obtained at a load of 40 N. As can be seen, the film thickness of VMWO increased with increasing entrainment speed and decreasing temperature. Similar profiles were obtained

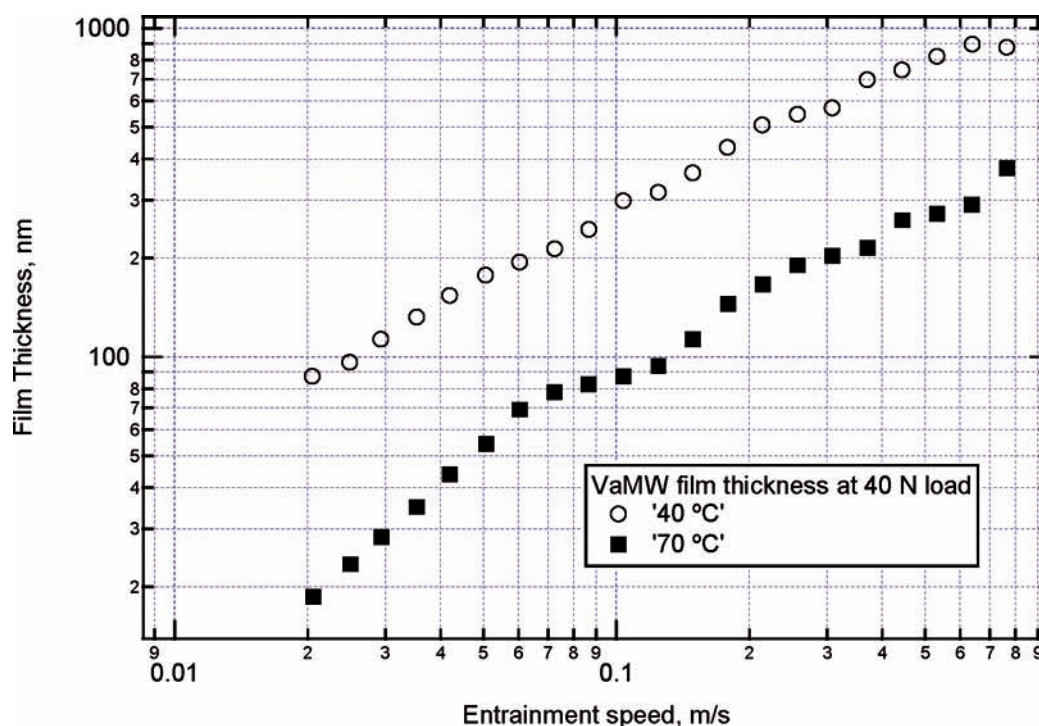


Figure 3. Effect of entrainment speed and temperature on film thickness.

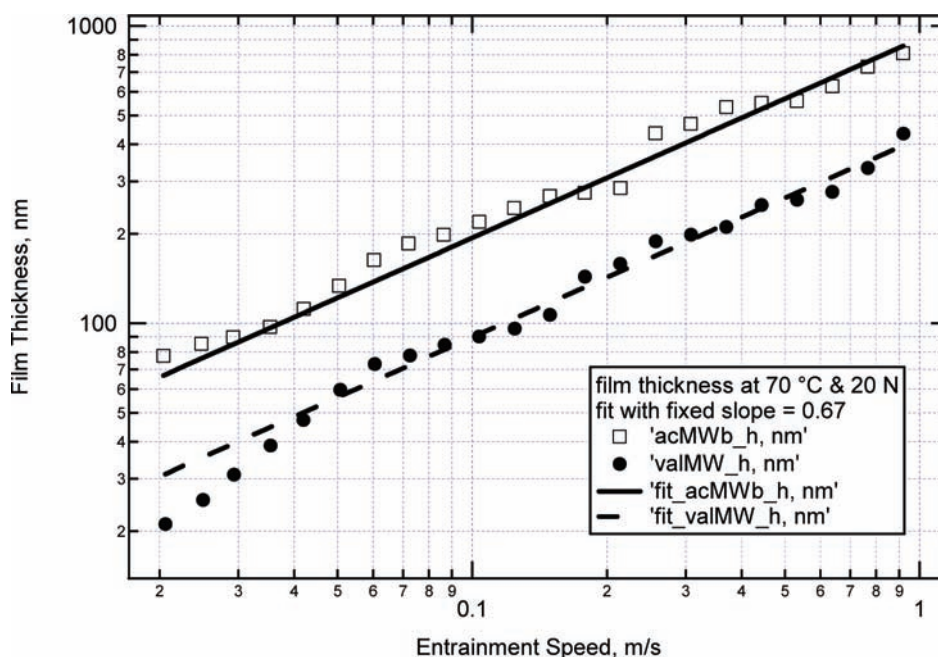


Figure 4. Effect of milkweed polyhydroxy ester chemical structure on measured versus predicted elastohydrodynamic film thickness.

for the film thickness of AMWO as a function of entrainment speed and temperature.

The effect of load (10, 20, 30, and 40 N) on the film thickness of VMWO and AMWO was investigated at various temperatures. The data (not included) clearly showed that the film thickness is independent of applied load. This observation was consistent with that generally observed for lubricating oils, which display little or no change with varying load.¹⁷

The effect of the chemical structure of milkweed derivatives on film thickness is illustrated in Figure 4, where film thickness data for milkweed AMWO and VMWO are compared. The points in Figure 4 are measured film thickness data at 20 N of load, at 70 °C. Examination of the data in Figure 4 clearly shows that at both temperatures, AMWO produces a much thicker film than VMWO. Similar results were obtained for these two oils at other temperatures. The difference in the film-forming properties

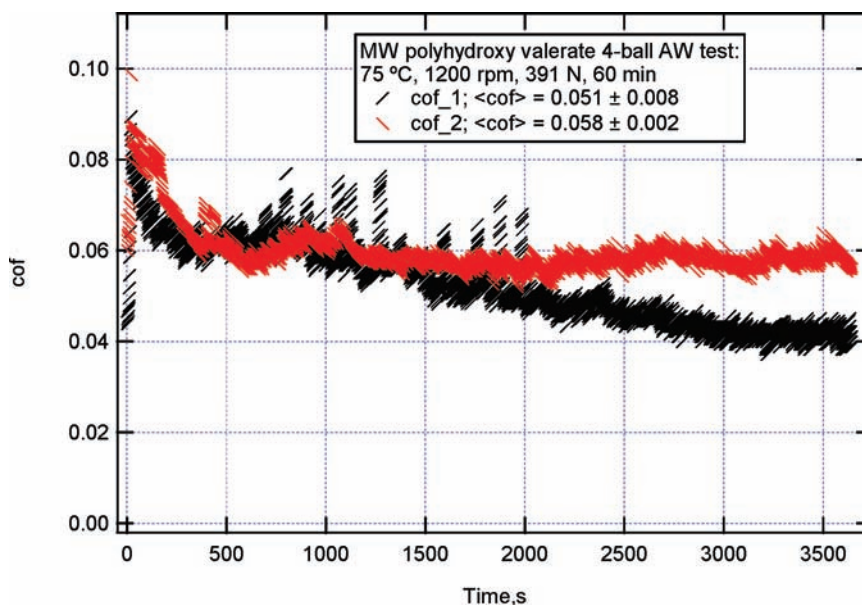


Figure 5. Time versus COF data for VMWO from repeat 4-ball AW measurements.

between these two oils is related to their difference in chemical structure. These two milkweed derivatives differ in the chain length of the carboxylic acid substituents on the polyhydroxy MWO. The longer carboxylate groups in the polyvalerates relative to those in the polyacetate led to a dramatic difference in the density and viscosity between these two materials (Tables 1 and 2). As shown in Tables 1 and 2, both the viscosity and the density of HMWO derivatives decreased due to esterification of the hydroxyl groups. In addition, both the viscosity and density of the esterified MWOs were functions of the chain length of the substituent groups. Both properties also decreased with increasing chain length, but the decrease in viscosity was the more dramatic. Viscosity and entrainment speed are the two major parameters affecting lubricant oil film thickness and can be used to predict film thickness using the Hamrock–Dowson (H-D) relationship.²⁸ Predicted film thickness of AMWO and VMWO oils using the H-D equation is illustrated by the lines in Figure 4. Examination of the measured versus predicted film thickness data in Figure 4 reveals a number of interesting features. For AMWO at 70 °C, the measured and predicted values showed excellent agreement at all entrainment speeds. For VMWO at 70 °C, an excellent agreement between experimental and predicted film thickness was observed mainly in the high entrainment speed region, which also corresponds to high film thicknesses. In the low entrainment speed region, however, VMWO displayed a negative deviation, that is, the measured film thickness was smaller than that predicted by the H-D theory. Such deviations between measured and H-D-predicted EHD film thicknesses, in thin and ultrathin film regions, have been reported for a number of oils.^{17,29–32} Various mechanisms have been proposed to explain these deviations, but more work is needed to develop a comprehensive theory.

Friction and Wear. The friction properties of these fluids were investigated using a four-ball tribometer configured for antiwear evaluation according to ASTM method D 4172.¹⁴ In this method, a steel ball is loaded (392 N) against three balls and rotated (1200 rpm) while completely immersed in the test lubricant maintained at 75 °C. During the test, which lasts 60 min, the frictional torque, temperature, load, and speed are continuously

monitored and recorded. At the end of the test, the WSD on the three balls are measured parallel and transverse to the wear direction, and the six measurements are averaged. The recorded frictional torque and load were used to calculate the COF using the procedure outlined in ASTM method D5183-95.¹⁵ Two tests were conducted on each test lubricant, and the resulting COF and WSD values from each measurement were averaged and used in further analysis.

An example of COF versus time data from a repeat measurement on a test lubricant is illustrated Figure 5. The data in Figure 5 are for neat VMWO. As shown in both measurements, the COF displayed an initial sharp increase and decrease. This was followed by a more or less steady-state value from about 500 s until the end of the test. The average and standard deviation of the COF values in the steady-state region of the repeat measurements for this lubricant were 0.051 ± 0.008 and 0.058 ± 0.002 . These values were further averaged and used in data analysis.

The corresponding WSD data from each of the two tests (six measurements per test) on VMWO gave the following average and standard deviation WSD values: 0.737 ± 0.058 and 0.819 ± 0.033 . These average WSD values as well as those from the other milkweed ester oils were identical within 1 standard deviation, so they were further averaged and used in analysis.

The average and standard deviation COF and WSD values of the milkweed polyhydroxy esters investigated here are summarized in Table 5. Examination of the COF results indicates that the three polyacyl derivatives displayed similar COF values within 1 standard deviation. These values were within the range of 0.04–0.11 reported for unformulated seed oils.²⁵ However, close comparison indicates that the COF values of the milkweed polyacyl esters are lower than those of commodity oils that have structures similar to milkweed (e.g., SBO, 0.08; CAN, 0.07). In fact, the COF of the milkweed esters is close to the lower end of the literature range, which is populated by very few commodity oils such as castor (COF = 0.04).²⁵ The relatively lower COF of milkweed polyesters may have to do with their high polarity because of the presence of multiple ester groups in their structure. Ester groups are known to promote adsorption of oil

Table 5. COF and WSD of Milkweed Polyhydroxy Esters from Four-Ball Antiwear Tests

oil	(COF) ± SD	(WSD) ± SD (mm)
AMW	0.059 ± 0.008	0.576 ± 0.030
BMW	0.064 ± 0.014	0.622 ± 0.067
VMW	0.055 ± 0.005	0.778 ± 0.058

molecules to metallic surfaces, resulting in lower COF.³³ The presence of multiple ester groups in molecules, as in the case of the oils studied in this work, has been found to lead to a stronger adsorption and further lowering of COF.³⁴ This is attributed to possible binding of the oil molecules to multiple sites using more than one ester group. The relatively low COF results shown in Table 5 for the oils studied in this work are consistent with expectation based on multiple binding of these molecules to the friction surfaces.

It is interesting to note that, even though these oils had similar degrees of esterification, they differ in the structure of the ester group, particularly the chain length. One might expect, on the basis of steric or other considerations, that the three polyesters would have to overcome various degrees of barriers to attain multiple bonding on the metal surface. The fact that they all had similar COF might be an indication that a partial multiple bonding is responsible for the observed COF values. Such partial multiple bonding can be attained by all three esters to an equal degree and does not require overcoming steric or other barriers. However, if a complete multiple bonding was responsible, the COF values would have been different as a function of structural or other barriers to adsorption.

Examination of the WSD data in Table 5 shows that the values for the milkweed polyesters are within the reported range for commodity oils (0.51–0.87 mm).²⁵ Comparison of the values for the three esters indicates that there was no difference in WSD values between AMWO and BMWO within 1 standard deviation. However, the WSD value for VMWO was much higher than the other two. VMWO oil has the lowest viscosity among the three, which might have contributed to its relatively higher WSD.

AUTHOR INFORMATION

Corresponding Author

*Phone: (309) 681-6341. Fax: (309) 681-6524. E-mail: Rogers.HarryOkuru@ars.usda.gov.

DISCLOSURE

Names are necessary to report factually on available data. The USDA neither guarantees nor warrants the standard of the product, and the use of the name by USDA implies no approval of the product to the exclusion of others that may also be suitable.

ACKNOWLEDGMENT

We express our gratitude to Mark Klokkenga for the kinematic viscosity measurements, Andrew J. Thomas for the dynamic viscosity measurements, Amber Durham for the pour points, cloud points, and RPVOT measurements, and Linda Cao for the film thickness, friction, and wear measurements.

REFERENCES

(1) Berkman, B. Milkweed – a war strategic material and a potential industrial crop for sub-marginal lands in the United States. *Econ. Bot.* **1949**, *3*, 223–239.

(2) Rusch gen Klaas, M.; Warwel, S. Chemoenzymatic epoxidation of unsaturated fatty acid esters and plant oils. *J. Am. Chem. Soc.* **1996**, *73*, 1453–1457.

(3) Pagès-Xatart-Parès, X.; Bonnet, C.; Morin, O. Synthesis of new derivatives from vegetable oil methyl esters via epoxidation and oxirane opening. In *Recent Developments in the Synthesis of Fatty Acid Derivatives*; Knothe, G., Derkson, J. T. P., Eds.; AOCS Press: Champaign, IL, 2000; pp 141–156.

(4) Harry-O'kuru, R. E.; Holser, R. A.; Abbott, T. P.; Weisleder, D. Synthesis and characteristics of polyhydroxy triglycerides from milkweed oil. *Ind. Crops Prod.* **2002**, *15*, 51–58.

(5) Harry-O'kuru, R. E.; Gordon, S. H.; Biswas, A. A facile synthesis of aminohydroxy triglycerides from new crop oils. *J. Am. Oil Chem. Soc.* **2005**, *82*, 207–212.

(6) Harry-O'kuru, R. E. Sunscreen reagents from unsaturated waxes and triglycerides. U.S. Patent 7,351,403, April 1, 2008.

(7) AOCS *Official Methods and Recommended Practices of the AOCS*, 5th ed.; AOCS Press: Champaign, IL, 1997; Method Tq 1a-64.

(8) American Society for Testing Materials. ASTM D 445-97: Standard test method for kinematic viscosity of transparent and opaque liquids (the calculation of dynamic viscosity). In *Annual Book of ASTM Standards*; ASTM: Philadelphia, PA, 1997.

(9) Biresaw, G.; Bantchev, G. Effect of chemical structure on film-forming properties of seed oils. *Synth. Lubr.* **2008**, *25*, 159–183.

(10) American Society for Testing Materials. ASTM D 2270-93: Standard practice for calculating viscosity index from kinematic viscosity at 40 and 100 °C. In *Annual Book of ASTM Standards*; ASTM: Philadelphia, PA, 1998.

(11) American Society for Testing Materials. ASTM D 97-96a: Standard test method for pour point of petroleum products. In *Annual Book of ASTM Standards*; ASTM: Philadelphia, PA, 1996.

(12) American Society for Testing Materials. ASTM D 2500-99: Standard test method for cloud point of petroleum products. In *Annual Book of ASTM Standards*; ASTM: Philadelphia, PA, 1999.

(13) American Society for Testing Materials. ASTM D 2272-98: Standard test method for oxidation stability of steam turbine oils by rotating pressure vessel. In *Annual Book of ASTM Standards*; ASTM: Philadelphia, PA, 1998.

(14) American Society for Testing Materials. ASTM D 4172-94: Standard test method for wear preventive characteristics of lubricating fluid (four-ball method). In *Annual Book of ASTM Standards*; ASTM: Philadelphia, PA, 2002; Vol. 05.02, pp 752–756.

(15) American Society for Testing Materials. ASTM D 5183-95: Standard test method for determination of the coefficient of friction of lubricants using the four-ball wear test machine. In *Annual Book of ASTM Standards*; ASTM: Philadelphia, PA, 2002; Vol. 05.03, pp 165–169.

(16) Johnston, G. J.; Wayte, R.; Spikes, H. A. The measurement and study of very thin lubricant films in concentrated contacts. *Tribol. Trans.* **1991**, *34*, 187–194.

(17) Biresaw, G. Elastohydrodynamic properties of seed oils. *J. Am. Oil Chem. Soc.* **2006**, *83*, 559–566.

(18) Harry-O'kuru, R. E.; Carriere, C. J. Synthesis, rheological characterization and constitutive modeling of polyhydroxy triglycerides derived from milkweed oil. *J. Agric. Food Chem.* **2002**, *50*, 3214–3221.

(19) Lawate, S. S.; Lal, K.; Huang, C. Vegetable oils — structure and performance. In *Tribology Data Handbook*; Booser, E. R., Ed.; CRC Press: New York, 1997; pp 103–116.

(20) Adhvaryu, A.; Erhan, S. Z. Epoxidized soybean oil as a potential source of high temperature lubricants. *Ind. Crops Prod.* **2002**, *15*, 247–256.

(21) Whistler, R. L.; BeMiller, J. N. Factors influencing gum costs and application. In *Industrial Gums, Polysaccharides and Their Derivatives*; Whistler, R. L., Ed.; Academic Press: 1959; pp 1–13.

(22) Jonsson, U. J. Lubrication of rolling element bearings with HFC-polyester mixtures. *Wear* **1999**, *232*, 185–191.

(23) Gee, M. L.; McGuiggan, P. M.; Israelachvili, J. N. Liquid to solid like transitions of molecularly thin films under shear. *J. Chem. Phys.* **1990**, *93*, 1895–1906.

- (24) Sendjarevic, I.; McHugh, A. J. Effects of molecular variables and architecture on the rheological behavior of dendritic polymers. *Macromolecules* **2000**, *33*, 590–596.
- (25) Wood-Adams, P. The effect of long chain branches on the shear flow behavior of polyethylene. *J. Rheol.* **2001**, *45*, 203–210.
- (26) Harry-O'kuru, R. E.; Isbell, T. A.; Weisleder, D. Synthesis of estolide esters from *cis*-9-octadecenoic acid estolides. *J. Am. Oil Chem. Soc.* **2001**, *78*, 219–222.
- (27) Adhvaryu, A.; Liu, Z.; Erhan, S. Z. Synthesis of novel alkoxy-lated triacylglycerols and their lubricant base oil properties. *Ind. Crops Prod.* **2005**, *21*, 113–119.
- (28) Hamrock, B. T.; Dowson, D. *Ball Bearing Lubrication: The Elastohydrodynamics Elliptical Contacts*; Wiley: New York, 1981.
- (29) Guangteng, G.; Spikes, H. A. The control of friction by molecular fractionation of base fluid mixtures at metal surfaces. *Tribol. Trans.* **1997**, *40*, 461–469.
- (30) Spikes, H. A. Direct observation of boundary layers. *Langmuir* **1996**, *12*, 4567–4573.
- (31) Spikes, H. A. The rheology of very thin lubricant films. Solid-solid interactions. In *Conference Proceedings of the Royal Society—Unilever indo—UK Forum in Materials Science and Engineering*; London, U.K., 1996; pp 334–351.
- (32) Biresaw, G.; Bantchev, G. Effect of chemical structure on film-forming properties of seed oils. *Synth. Lubr.* **2008**, *25*, 159–183.
- (33) Jahanmir, S.; Beltzer, M. Effect of additive molecular structure on friction coefficient and adsorption. *J. Tribol.* **1986**, *108*, 109–116.
- (34) Biresaw, G.; Adhvaryu, A.; Erhan, S. Z.; Carriere, C. J. Friction and adsorption properties of normal and high oleic soybean oils. *J. Am. Oil Chem. Soc.* **2002**, *79*, 53–58.